Wind Energy

WILEY

REVIEW ARTICLE OPEN ACCESS

Measurement Technologies for Tribological Monitoring of Tilting-Pad Journal Bearings: A Review

G. Nicholas | R. S. Dwyer-Joyce

The University of Sheffield, Sheffield, United Kingdom

Correspondence: G. Nicholas (gary.nicholas@sheffield.ac.uk)

Received: 26 March 2025 | **Revised:** 4 July 2025 | **Accepted:** 20 September 2025

Funding: This work is supported by the Centre for Postdoctoral Development in Infrastructure, Cities and Energy and the Engineering and Physical Sciences Research Council (EP/W037009/1 and EP/X528493/1).

Keywords: oil film thickness | pressure | review article | sensing technologies | sensing technologies | tilting-pad journal bearing | wind turbine sliding bearings

ABSTRACT

Recently, there has been an uptrend in interest in adopting tilting-pad sliding bearings for wind turbine main bearing applications. Manufacturers have opted for designs with interchangeable pads, emphasizing the importance of ease of maintenance. However, effective monitoring technologies are essential to identify pads that require replacement. Additionally, full-scale testing of these large bearings is costly, necessitating carefully planned instrumentation to maximize data yield. Consequently, this article explores the available sensing technologies for performance monitoring of tilting-pad sliding bearings. Parameters are critically evaluated and key findings summarized in a table that includes each parameter's measurement methods, limitations, accuracy, and technology readiness level. Given current limitations, a multisensor approach is recommended as integrating multiple sensing methods to measure a range of bearing parameters can maximize data yield and reduce uncertainty.

1 | Introduction

Global energy demand is projected to increase in the coming decade, growing by an annual rate of 3.4% in the next 2 years primarily due to electrification of the transport and residential sectors as well as growing demand from data centers, AI, and cryptocurrencies [1]. Emerging markets are also expected to contribute up to 85% of the additional energy demand [1, 2]. ExxonMobil has projected that global electricity demand will double and energy demand for industry will increase by one-fifth by 2050 [3].

To satiate global energy demand from renewable sources, wind capacity is expected to continue to trend upwards. In 2023, 54 countries reported an increase in wind power capacity. The GWEC has recently revisited its 2030 growth forecast and increased it by 10% up to 1210 GW [4]. In Europe, 18.3 GW of new wind power capacity was installed in 2023, with 260 GW forecasted to be in the pipeline by 2030 in an attempt to meet Europe's 2030 climate and energy targets [5]. As wind capacity increases, wind turbine designs have trended larger in size [6, 7] with an average rotor diameter projected to reach 270 m in 2030 [6]. The increase in size has been suggested to have the highest impact in lowering the levelized cost of energy for offshore wind turbines [8].

Wind turbine drivetrains employ bearings to facilitate frictionless rotation and support loading. Conventionally, these bearings are of the rolling element variant, which operate through the principles of elasto-hydrodynamic lubrication [9, 10]. For wind turbine main shaft bearings, failures as high as 30% have been reported [11]. A recent study found that 22%–25% of the main bearings fail at year 20 [12, 13]. Of the failed bearings, a common failure mechanism was found to be spalling, suggested

TABLE 1 | Publicly available data on emerging wind turbine sliding bearing designs.

Affiliation	Bearing configuration	Type of pads	Interchangeable pads?	Type of pad coating	Targeted bearing
Siemens AG [15]	Radial and axial pads	Not stated	Yes	Not stated	Main bearing
Daido Metal [16]	Radial and axial pads	Tilting	Yes	PEEK with filler	Main bearing
Waukesha Bearings [17]	Radial and axial pads	Tilting	Yes	PEEK	Main bearing
Renk GmbH [18]	Radial pads	Tilting	Yes	Not stated	Main bearing
Miba AG [19]	Radial and axial pads	Tilting	Yes	Not stated	Gearbox bearing
RWTH Aachen [20]	Double conical pads	Stationary but deformable	Yes	Soft metal	Main bearing

to be from surface concentrations or insufficient lubrication. In addition, main bearings have also been reported to fail due to slip-induced micro-pitting [14]. Rolling contact fatigue thus is still considered to be one of the predominant failure mechanisms of main bearings. Additionally, as wind turbines grow larger, it is more challenging to manufacture bearings at the required size with the existing manufacturing setup and transport the components to the site.

Consequently, the wind industry is facing a paradigm shift away from rolling element variants toward sliding bearings that are predominantly used in higher rotational speed applications such as hydropower plants, marine propellers, and jet engines. Sliding bearings fundamentally operate through hydrodynamic lubrication, where the lubricant is entrained into the contact through rotational motion, and the shearing of the lubricant ensures low friction between the sliding surfaces. Patents for such designs have emerged as early as 2017 [15] and despite being a relatively new niche, companies such as Daido Metal [16], Waukesha Bearings [17], Renk GmbH [18], and Miba AG [19] have already established a presence within the market. A notable academic contribution comes from RWTH Aachen, which proposes a flexible, conical-shaped sliding bearing design for wind turbine main bearings [20].

Table 1 contrasts the various sliding bearing designs from different companies, based on openly available data. Most companies opted for two separate sets of pads, one set to react to radial loads while the other for axial loading. This circumvents potential issues when scaling for larger capacity turbines as the axial and radial loadings do not increase proportionally with power capacity [21]. Tilting pads are employed to allow pads to attain their optimum load-carrying positions during operation, and pads have interchangeability to facilitate maintenance. Limited information is found on pad coating material. Daido and Waukesha employ polymer-based pads while no information can be found for Renk and Miba. RWTH Aachen remains the outlier, opting for a soft metal-based coating for their unique flexible conical bearing design. Apart from Miba, all the aforementioned product offerings are targeted at wind turbine main bearings.

Moreover, all companies have opted for interchangeable pads, emphasizing the importance of ease of maintenance in their product offerings. However, this is only one aspect of the challenge, as effective monitoring technologies are essential to identify which pads require replacement. Additionally, there is limited publicly available information on the performance of sliding bearings under the low speed, transient loading conditions of wind turbines. Sliding bearing test programs, particularly when conducted at full scale, can be costly and, as such, yield from these tests need to be maximized. Consequently, this article explores all the suitable sensing techniques available for monitoring and evaluation of wind turbine sliding bearings.

The novelty of this study includes the following:

a. A critical review of sensing techniques based on their advantages, limitations, accuracy, and technology readiness levels (TRLs) for tribological monitoring of wind turbine sliding bearings

b. A market survey compiling publicly available data on emerging wind turbine sliding bearing designs

c. A discussion of trends in the literature, known challenges, and potential mitigation strategies

Despite the study focusing on tilting-pad journal bearings, the monitoring methods can typically be adapted for plain journal bearing applications.

2 | Sliding Bearing Performance Parameters

Sliding bearing differs from rolling element bearing both in design and operation. As such, measurement techniques applied for roller bearings may not be suitable for sliding bearings. Tilting-pad sliding bearings function through hydrodynamic lubrication. Lubricant is entrained between the sliding shaft and tilting pads through the rotational motion of the shaft, enabling low friction operation with a friction coefficient between 0.005 and 0.015 [22]. The lubricant film

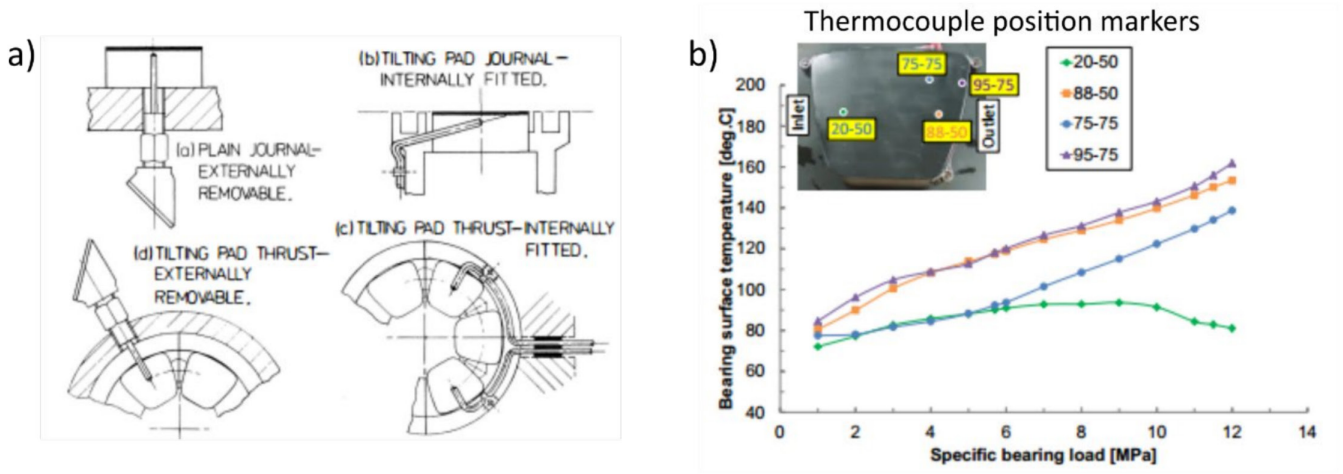

FIGURE 1 | a) Thermocouple installation methods [32] and b) variation of bearing surface temperature with increasing load [37].

thickness generated ranges between 5 and 200 μm with contact pressures in the MPa range. For wind turbine main shaft application, the film generated is likely to be much lower, i.e., 5–40 μm due to the low rotational speed and higher bearing load.

Conversely, rolling element bearings function through elastohydrodynamic lubrication with a much lower coefficient of friction of between 0.001 and 0.005 [23]. The lubricant film formed between the rolling contacts is also much thinner, between 1 and 5 μm, with higher contact pressures (GPa range). For sliding bearings in wind applications, start-up is particularly challenging as the frictional torque is highest, which poses an elevated risk of wear between sliding surfaces. Industrial solutions include sacrificial, low-friction polymer, or soft metal coating on pads and/or jacking lubricant into the shaft/pad interface to reduce boundary friction [24].

Based on the literature, the following parameters are commonly used to evaluate the performance of tilting-pad journal bearings:

- Temperature [25–40]
- Lubricant pressure [41–46]
- Lubricant film thickness [47–64]
- Shaft center displacement [65–68]
- Bearing vibration [69–73]
- Acoustic emission [74–80]

Details pertaining to the capabilities, limitations and practicalities for each measurement parameter are summarized in the following subsections.

2.1 | Temperature

Historically, temperature measurements have been a common way of detecting faults in machine components, as rapid temperature changes are highly correlated with failures [25–28]. Such an approach has been successfully used for anomaly identification [28–31] in sliding bearings. The temperature increase beyond operating norm is a consequence of the frictional heat generated from asperity contacts, usually indicative of lubrication issues.

Measurements are commonly acquired either through thermocouples (J/K-type) or resistance temperature detectors (RTDs). Figure 1a illustrates the various thermocouple installation methods for soft metal tilting pads [32]. Details pertaining to their positioning, installation, and threshold settings for Babbitt-lined sliding bearings are comprehensively described in [32, 33].

As polymer pad coatings alter the pad's thermal conductivity, methods established for white metal sliding bearings may not be suitable for polymer-coated variants. Despite this, multiple literatures exist demonstrating its success on polymer-faced sliding bearings [34–39]. A sample of such measurement is illustrated in Figure 1b. Lubricant film temperature provides the fastest response and is independent of coating; however, it typically necessitates machining of pad to accommodate sensors. Measuring pad metal temperature maintains the integrity of the sliding surface, but this incurs an error between the surface temperature and measured temperature.

The advantages of thermocouples are low cost and simplicity to implement. Alarm thresholds can be assigned to detect anomalies, and preventive maintenance can be scheduled when temperatures exceed the norm. However, limited information can be gained, and numerical modelling [40] is often required to further infer bearing parameters such as displacement angle, eccentricity, and oil film thickness. Consequently, temperature sensors are often employed in addition to other sensors during testing or monitoring of sliding bearings.

2.2 | Lubricant Pressure

Measurement of lubricant pressure is achieved through pressure transducers which convert applied pressure into electric signals. Structurally, they typically consist of an elastic material designed to deform under pressure and an electrical device, which senses the deformation and converts it to electrical signals. The most common types are capacitive, piezoresistive, piezoceramic pressure transducers, and bourdon-gauges as illustrated in Figure 2.

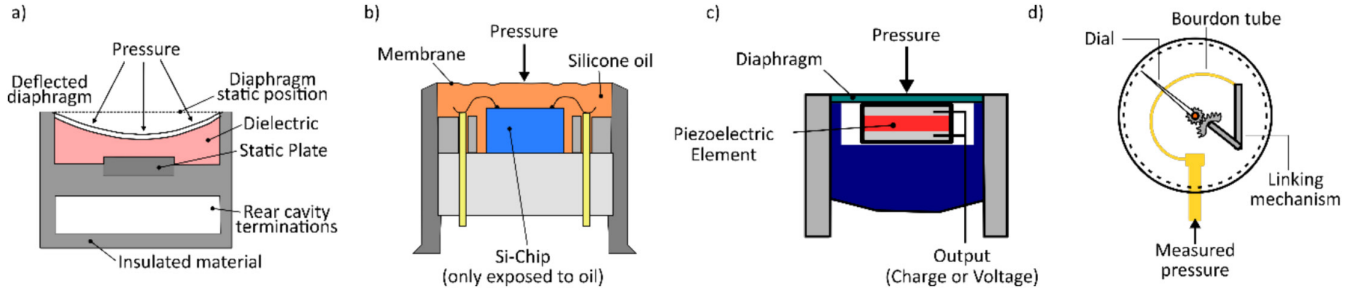

FIGURE 2 | Types of pressure measurement devices: a) Capacitive, b) Piezoresistive, c) Piezoelectric pressure transducers, and d) Bourdon-gauge.

Historically, researchers have utilized both piezoresistive [41, 42] and piezoceramic [43] pressure transducers and bourdon gauges [44] for tilting-pad test rig instrumentation. Measurement parameters range from oil inlet pressures [44] to pressure distribution across individual tilting pads [41–43]. The latter is of higher value but with the increased instrumentation challenge of embedding sensors either in the tilting pads [41] or within a hollow shaft through a slip ring [43].

No justification can be found on pressure transducer type selection, with some publications [45, 46] opting to omit the pressure transducer type used. However, utilizing the inappropriate pressure transducer for testing is likely to result in poor measurements. Piezoceramic pressure transducers, typically used to measure transient pressure in explosions, do not require an external excitation, have extremely high sensitivity, and are insensitive to electromagnetic interference. However, they are also sensitive to vibrations and temperature fluctuations. Conversely, piezoresistive variants are less sensitive to temperature fluctuations (typically with integrated temperature compensation), possess good sensitivity and responsiveness but require external power. For wind turbine tilting-pad main bearings, which operate at a maximum of 20 RPM, with large temperature fluctuations across the hot and cold seasons, the latter is deemed more suitable and cost effective.

2.3 | Lubricant Film Thickness

As separation of sliding surfaces is crucial in maintaining low friction and consequently preventing wear during bearing operation, direct measurement of lubricant film thickness remains the most desirable parameter. Film thickness measurement informs on the bearing lubrication regime during operation. However, this is difficult as the films are typically less than 50 μm and the oil film is entrapped within an interface of a component. As a consequence, no standardized method for measuring sliding bearing oil film exists to date.

Multiple measurement techniques have been developed, which include eddy current, capacitance, and ultrasound. Such technologies are widely used in research and product testing; however, they are rarely implemented beyond that.

2.3.1 | Ultrasound Method

Ultrasound is mechanical vibrations propagating within a medium beyond the audible range of human hearing (> 20 kHz). Piezoelectric ultrasonic sensors bonded onto a component generate and receive wave reflections. The reflected signals, if incident on the lubricant film, will contain information on the film thickness [47, 48]. This has successfully been exploited for hydrodynamic oil film thickness measurement in mechanical seals [49], thrust bearings [50], piston skirt internal combustion engines [51], and journal bearings [52, 53].

The primary advantage of the technique lies in its noninvasive capabilities, relative low cost, good measurement range (1–50 μm) and accuracy, and universality (method applicable to both soft metal and polymer coated pads). Measurement error is highly setup-dependent and will be influenced by sensor bandwidth and calibration, signal noise, and processing algorithm used. Consequently, the method requires specialist understanding as well as computational and data storage capabilities if high sampling rates are desired (for accurate measurements at 1–5 μm). Instrumentation is also complex, as illustrated in Figure 33; however, this is comparable to other film measurement techniques. Additionally, calibration will be required when instrumenting and measuring from multilayered tilting pads, as shown in Figure 3a.

2.3.2 | Electrical Capacitance Method

Capacitive, noncontact gap sensors operate through parallel-plate theory where the capacitance change within the projected field is influenced by the measurement area, electrical properties of the material within the field, and the gap between the sensor and the ferrous measurement target. They have been successfully employed to measure hydrodynamic oil film thickness formed in tilting-pad journal bearings [54–58]. Both stationary pad and dynamic shaft installation options have been pursued, as illustrated in Figure 4. The former is easier; however, instrumentation disrupts pad sliding geometry and does not provide circumferential film thickness measurements across all the tilting pads. As the film measurements require the relative permittivities of the materials between the sensor and target, the method is more suited for soft metal-coated tilting pad bearings if instrumented within the shaft. Measurements are still possible for polymer-coated bearings, provided that coating thickness is known (negligible deformation under load, no wear, uniform coating thickness across) [57]. Capacitance sensors possess a good measurement range (50–500 μm) and resolution (< 1 nm) [59]. However, the sensors are costly, and any changes to the relative permittivities of the lubricant (contamination, water ingress) and coating (wear, damage) will introduce measurement error.

2.3.3 | Eddy Current Method

An eddy current sensor, as illustrated in Figure 5a, consists of a coil that, when subjected to an alternating current, generates an alternating electromagnetic field. When this field cuts through a ferrous object, an eddy current is induced, which alters the impedance of the sensor's electrical circuitry. The change in impedance is then converted to gap/lubricant film thickness.

As with capacitance probes, they are small-sized, noncontacting, have good accuracy and range with the added benefit of not being affected by the electrical properties of the material within the measurement zone. Modern eddy current sensors also typically come with in-built temperature compensation [60]. As such, they are particularly suited for lubricant film thickness measurement in metal-faced sliding bearings [61].

For polymer-coated bearings, when instrumented within the shaft, the measured gap contains both the thickness of the lubricant and the polymer coating. As such, thickness of the coating needs to be known to convert gap measurements into lubricant film thickness. Consequently, all of the previous literatures

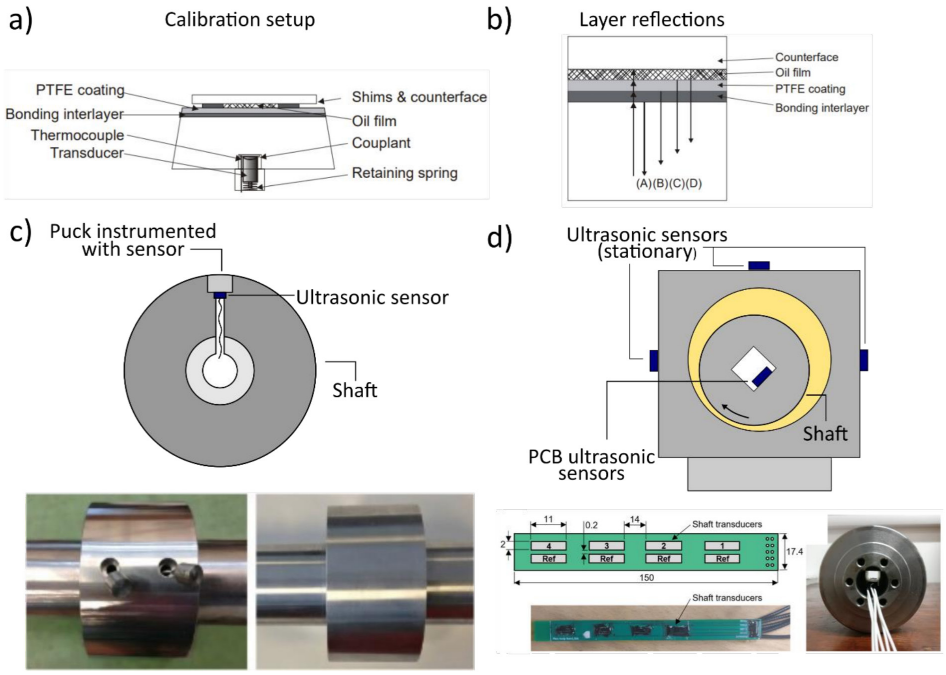

FIGURE 3 | a) Ultrasonic sensor calibration setup for b) multilayered tilting pads [50] and instrumentation methods for journal bearing, c) hollow shaft with instrumented puck [52], and d) printed circuit board integrated sensors [53].

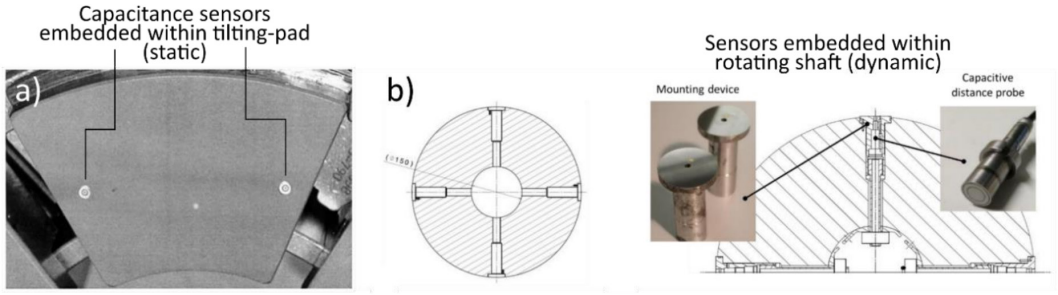

FIGURE 4 | Capacitance sensors embedded within a) tilting-pad [54] and b) hollow shaft [58].

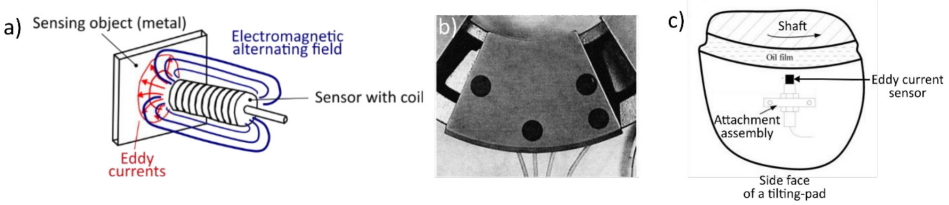

FIGURE 5 | Eddy current sensor a) internal structure and instrumentation methods: b) embedded within [61] and c) attached to the side of a tilting-pad [62].

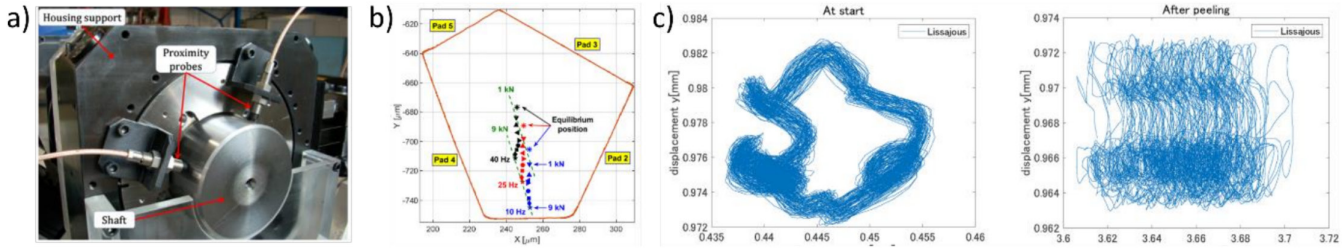

FIGURE 6 | a) Eddy current setup for b) shaft displacement measurements [81]. c) change in shaft displacement pattern with bearing damage [83].

[61–64] have opted for pad-side instrumentation. Such instrumentation (Figure 5b), especially for polymer-coated pads, would affect the hydrodynamic film formation due to difference in stiffness between the sensor bulk material and the pad coating. Sensor instrumented on the side faces of the tilting-pad (Figure 5c) circumvents this, however, does not exactly measure the hydrodynamic film thickness that forms within the tilting-pad.

One major issue affecting eddy current measurements is electrical runout. This error arises because of the variation in the electrical properties across a sensing object [81–83], that is, around the shaft circumference. The exact root cause is not well researched [84], with possible causes attributed to structural inhomogeneity, surface roughness, residual magnetism and residual stresses present within the measurement target [84], which could incur errors up to 20 μm. As such it is critical that these effects are mitigated through experimental calibration and pretest treatments such as demagnetizing the measurement object and ensuring a roughness of $< 0.3\,\mu m$.

2.4 | Shaft Displacement (Proximity Probes)

Where it is unfeasible to modify the sliding bearing to accommodate eddy current displacement sensors, two or more eddy current sensors can be positioned at distinct locations around the shaft circumference (Figure 6a) to measure shaft displacement [65, 66]. Bearing eccentricity and oil film thickness can subsequently be inferred from the measurements. Additionally, the shaft displacement in the X and Y axes can be utilized for condition monitoring purposes as shown in Figure 6c. The shaft displacement pattern deviates from the norm when the journal bearing is damaged [67], and algorithms can be written to automatically detect this. This technique has also been commercialized [68]. However, it is prudent to note that for measurements to yield meaningful results, thermal expansion of components and vibration need to be accounted for.

2.5 | Vibration

Component vibration is commonly measured for nondestructive purposes. This is typically achieved through the use of accelerometers, which convert tiny surface deflections (vibrations) into electric voltage.

In tilting-pad journal bearings, accelerometers are often attached to the bearing housing, deployed alongside eddy current shaft displacement sensors and load cells to measure the bearing dynamic coefficients (damping, stiffness, and virtual mass) [69–71]. Their primary advantage lies in their capability to characterize dynamic coefficients and diagnose dynamic operational issues such as rotor imbalance [72] and pad flutter [50]. Through monitoring the bearing natural frequency and damping ratio, it is also feasible to identify bearing starvation [73].

2.6 | Acoustic Emissions

Acoustic emissions (AEs) are sound waves generated as a loaded material redistributes its internal stresses [74]. These are measured with a broad-band piezoelectric AE sensor as shown in Figure 7a and b. The generated bursts (Figure 7c) have a spectral content of typically less than 1 MHz. Their primary advantage lies in their high sensitivity, enabling detection of acoustic bursts from asperity contacts and subsequently inferring the lubrication regime of the sliding contact [27, 75–79]. An active patent [80] exists for the instrumentation of AE sensors on sliding bearings for monitoring purposes.

Because AE sensors are often instrumented far away from the source of interest (sliding contact) [75–78], measurements often contain noise from undesired sources. Consequently, to maximize yield, advanced data processing techniques such as decomposition [75] and machine learning [27, 76, 77] algorithms are required. One of the challenges with AE sensors is the large amount of data generated as a consequence of the high sampling rates needed. Efficient postprocessing of these data will require adequate computational power, especially if employing advanced processing algorithms.

2.7 | Strain

Strain measurements are widely used to assess the stress state of a component. This is typically achieved using strain gauges, as illustrated in Figure 8a. Strain gauges measure changes in electrical resistance within their circuitry when subjected to strain. These resistance changes are then converted into strain values using a gauge factor.

Despite their widespread adoption in many engineering applications, they are not commonly instrumented on journal bearings [85–87]. The most relevant approach [85], as shown in Figure 8b, utilizes strain gauges instrumented on the pivot pins of individual tilting-pads to measure surface strain of the pivot pins. The measured strain is then converted into radial pad loading through a calibration experiment. Disadvantages include delicate and time-consuming instrumentation. Additionally, for

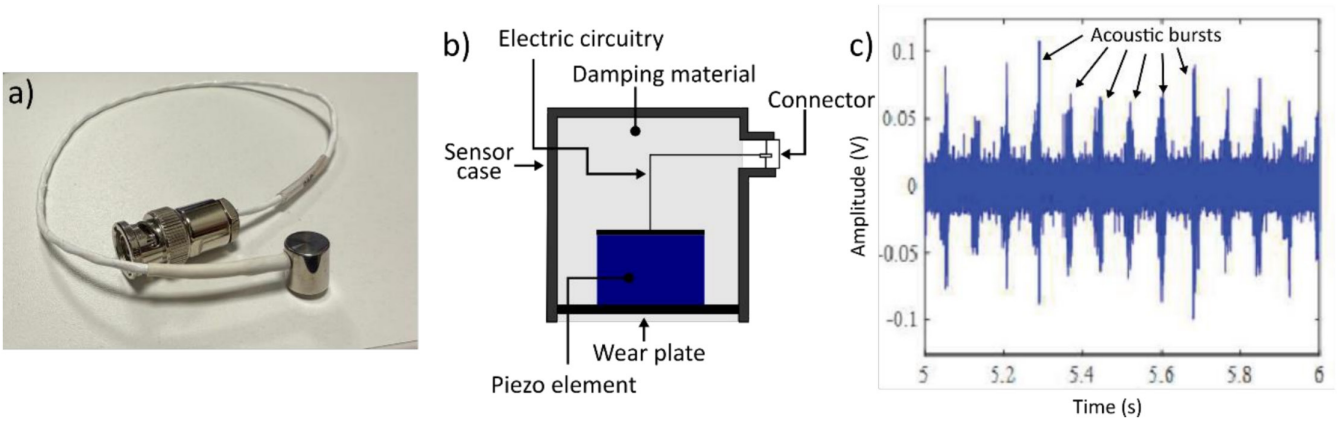

FIGURE 7 | a) Photo and b) internal structure of an AE sensor and c) a sample AE signal [75].

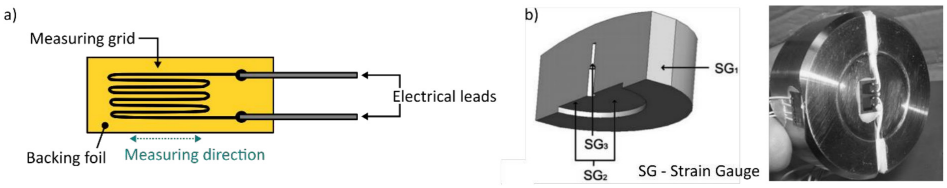

FIGURE 8 | a) Typical single-element strain gauge and b) strain gauge instrumentation on a pivot pins of a tilting-pad hydrogenator journal bearing [85].

reliable measurements, effects of bearing preload [86], lubricant ingress onto strain gauges and temperature fluctuations all need to be mitigated. Conversely, an expired patent [88] exists for using strain gauges to detect journal bearing failure. Strain gauges are installed on the bearing housing to measure fluctuations in frequency spectrum of the fluid film pressure. An alarm would then be assigned for shutdown when the fluctuations are excessive. In summary, the advantages of strain gauges are their low cost, simplicity, and widespread adoption for stress measurement. Challenges, however, include sensitivity to temperature fluctuations, calibration requirements to convert strain into meaningful loading, and a zero reference/datum requirement.

3 | Discussion

3.1 | Trends in Literature

Table 2 summarizes the various tilting-pad performance parameters, sensing techniques available to monitor them, their advantages, limitations, and development stage.

Based on available literatures, the most popular and well-established measurement is temperature, owing to its low cost, simplicity to implement, and interpret the results. Tilting-pad bearings are often specified with grooves to accommodate retrofitting of thermocouples or RTDs. While temperature data provide a basic indication of normal operation, its utility is limited unless combined with thermal models [40] to infer tribological parameters.

Conversely, despite being commonly utilized in engineering, strain is the least established method for tilting-pad journal bearing sensing. Strain gauges are possibly deemed not sensitive enough to measure the tiny surface strains resulting from the low hydrodynamic pressures in small-sized bearings. However, they have found success in large hydropower tilting-pad bearings and present an attractive adoption for large wind turbine main journal bearings. Strain gauges instrumented on the pivot pins of individual pads can inform on asymmetric pad loading and, with sufficient understanding of baseline normal strain values, be used to indicate abnormal operation for maintenance interventions. As demonstrated with thermocouples, bearing manufacturers can easily include grooves or features within their design to integrate strain gauges and elevate their product offerings.

3.2 | Rotating Versus Stationary Instrumentation

For any tilting-pad journal bearing testing or monitoring instrumentation, a decision needs to be made on whether to embed the sensors within the rotating shaft or onto the stationary components (tilting-pads, housing). Shaft-side instrumentation allows dynamic measurement around the bearing circumference and maintains the structural integrity of the bearing components. However, this typically involves more complex instrumentation and requires a solution to transmit data from rotating cables to stationary data loggers (i.e., slip ring, telemetry). Additionally, some measurements such as temperature are unsuitable for shaft-side instrumentation, while other sensors such as eddy current require additional calibration.

Stationary instrumentation either within or on the bearing subcomponents is easier to implement; however, it typically requires modifying the bearing to accommodate sensors and cables. This is usually not feasible for small-sized tilting-pad journal bearings but would be less of an issue for large-sized wind turbine

TABLE 2 | Summary of tilting-pad performance parameters and technologies available to measure them.

Parameter	Measurement technology	Advantages	Limitations	Accuracy	Technology readiness level
Temperature	Thermocouple (J/K-type)	Durable, faster response, wider temperature range	Binary output (temperatures within norm or not), requires thermal modelling to further extract tribological parameters	±1.5–2.5°C [89, 90]	TRL 7
	RTD	Linear output, better stability and repeatability		±0.5°C [90]	TRL 7
Lubricant pressure	Capacitive	Low power, durable	Nonlinear response, sensitive to vibration	±0.02% FSO [91]	—
	Piezoresistive	Linear output, vibration and dynamic pressure resistant, stable output	Temperature compensation required	<±2.0% FSO [92]	TRL5
	Piezoelectric	Low power, high sensitivity, suitable for high pressures and temperatures	Sensitive to vibration, only suitable for dynamic pressure measurements (measurement drifts)	<±1.0% FSO [93]	TRL5
Lubricant film thickness	Ultrasound	Preserves sliding geometry/does not affect hydrodynamic film formation, high measurement resolution	Requires specialist knowledge, accuracy dependent on setup and instrumentation	0.1%–10% FSO [52] (when compared with theoretical model)	TRL5
	Electrical capacitance	Free from electromagnetic interference	Requires prerequisite (dielectric permittivities), difficult to integrate within a slip ring assembly, instrumentation interferes with hydrodynamic film formation	±3% [54], <±0.03% FSO [59]	TRL5
	Eddy current	Insensitive to lubricant properties	Suffer from electrical runout, difficult to integrate within a slip ring assembly, instrumentation interferes with hydrodynamic film formation	0.1–0.16% FSO [61], <±0.2% FSO [60]	TRL5
Shaft displacement	Eddy current	Straightforward instrumentation, data easy to interpret	Thermal expansion of components and vibration affects measurement	—	TRL7

(Continues)

TABLE 2 | (Continued)

Parameter	Measurement technology	Advantages	Limitations	Accuracy	Technology readiness level
Vibration	Piezoelectric accelerometer	Able to characterize bearing dynamic parameters	Complex data processing, requires a suite of complementary sensors to characterize bearing dynamic parameters	—	TRL5
Acoustic emission	Piezoelectric	Possible to infer asperity contacts between sliding surfaces	Complex data processing, high computational power and data storage requirements	—	TRL5
Strain	Strain gauges	Able to monitor loading on individual tilting-pads	Fragile and time-consuming instrumentation, requires calibration to convert strain into load, sensitive to temperature and lubricant ingress	—	TRL3

Abbreviation: FSO, full-scale output.

main shaft tilting-pad journal bearings. This is especially feasible if manufacturers consider integrating sensors in their bearing design, as demonstrated with thermocouples for aero engine tilting-pad bearings.

3.3 | Challenges in Measuring Hydrodynamic Film Thickness

It is undeniable that optical interferometry [94] is the established standard for measuring elasto-hydrodynamic films in rolling bearings. However, no equivalent method exists for hydrodynamic sliding bearings. As light ceases to penetrate solids, its use is limited for testing and monitoring on unmodified bearings. Sound waves, governed by similar wave physics, circumvent this issue and present an attractive alternative, with good advancements made on the ultrasonic hydrodynamic film measurement method [47–53]. As the sliding contact geometry is not affected by ultrasonic instrumentation, the measurement has higher confidence.

Despite this, challenges exist with complex calibration and setup, issues also faced by other film measurement techniques such as eddy current and capacitance. Eddy current sensors suffer from electrical run-out, while electrical capacitance requires dielectric permittivities of the contact layers as measurement prerequisites. Further studies are required to quantify variability and improve sensor performance. Comparative studies evaluating these methods for oil film thickness measurement would also be valuable.

At its current state, for bearing product testing, where within budget, a multisensor measurement approach, employing multiple sensing technologies to measure various bearing parameters, would be the most sensible approach to reduce measurement uncertainty and maximize yield.

4 | Conclusions

Parameters to monitor the performance of tilting-pad journal bearings include temperature, lubricant pressure, film thickness, shaft displacement, vibration, AE, and strain. Temperature is by far the most established and adopted parameter, while strain is the least adopted. Among these, lubricant film thickness and pressure provide the most valuable insight, with multiple sensing technologies available. However, film thickness measurement techniques still face reliability and accuracy challenges. In contrast, lubricant pressure measurement is easier, with advancements in integrated piezoresistive or piezoelectric (IEPE) pressure sensors, with the former being more suitable for wind turbine main bearings. Shaft displacement is straightforward and well developed, while vibration and AE sensors offer alternative insights but require further interpretation to extract meaningful tribological parameters.

Given current limitations, a multisensor approach is recommended for bearing product testing where the budget allows. Integrating multiple sensing technologies to measure various bearing parameters can help minimize uncertainty and maximize data yield.

Acknowledgements

This work was supported by the Centre for Postdoctoral Development in Infrastructure, Cities and Energy (C-DICE). C-DICE is funded by the Research England Development Fund (www.cdice.ac.uk).

The project was also a collaboration with Offshore Renewable Energy Catapult (ORE Catapult), funded by the Engineering and Physical Sciences Research Council's Innovation Launchpad Network+ Researcher in Residence scheme (EP/W037009/1, EP/X528493/1).

Additionally, the authors would like to thank Mr. Wooyong Song from ORE Catapult for his technical input.

Data Availability Statement

Data sharing not applicable to this article as no datasets were generated or analysed during the current study.

References

1. International Energy Agency, "Electricity 2024: Executive Summary," (2025), https://www.iea.org/reports/electricity-2024/executive-summary.

2. Enerdata, "World Energy & Climate Statistics – Yearbook 2024," (2025), https://yearbook.enerdata.net/total-energy/world-consumption-statistics.html.

3. ExxonMobil, "Energy Demand Trends," (2025), https://corporate.exxonmobil.com/sustainability-and-reports/global-outlook/energy-demand-trends.

4. Global Wind Energy Council, "Global Wind Report 2024," (2025), https://www.gwec.net/reports/globalwindreport/2024.

5. WindEurope, "Wind Energy in Europe: 2023 Statistics and the Outlook for 2024–2030," (2025), https://windeurope.org/data/products/wind-energy-in-europe-2023-statistics-and-the-outlook-for-2024-2030/.

6. Statista, "Average Rotor Diameter of Onshore Wind Turbines Worldwide From 1980 to 2023, With a Forecast for 2030," (2025), https://www.statista.com/statistics/1085649/onshore-wind-turbines-average-rotor-diameter-globally/.

7. M. Bosnjakovic, M. Katinic, R. Santa, and D. Maric, "Wind Turbine Technology Trends," *Applied Sciences* 12, no. 17 (2022): 8653.

8. R. Wiser, J. Rand, J. Seel, et al., "Expert Elicitation Survey Predicts 37% to 49% Declines in Wind Energy Costs by 2050," *Nature Energy* 6 (2021): 555–565.

9. E. Hart, B. Clarke, G. Nicholas, et al., "A Review of Wind Turbine Main-Bearings: Design, Operation, Modelling, Damage Mechanisms and Fault Detection," *Wind Energy Science* 5, no. 1 (2020): 105–124.

10. J. Williams, *Engineering Tribology* (Cambridge University Press, 2005).

11. E. Hart, A. Turnbull, J. Feuchtwang, D. McMillan, E. Golysheva, and R. Elliott, "Wind Turbine Main-Bearing Loading and Wind Field Characteristics," *Wind Energy* 22, no. 11 (2019): 1534–1547.

12. J. Kenworthy, E. Hart, J. Stirling, et al., "Wind Turbine Main Bearing Rating Lives as Determined by IEC 61400–1 and ISO 281," (2025), https://www.nrel.gov/docs/fy23osti/86299.pdf.

13. E. Hart, K. Raby, J. Keller, et al., "Main Bearing Replacement and Damage – A Field Data Study on 15 Gigawatts of Wing Energy Capacity," (2025), https://www.nrel.gov/docs/fy23osti/86228.pdf.

14. M. Kotzalas and G. Doll, "Tribological Advancements for Reliable Wind Turbine Performance," *Philosophical Transactions of the Royal Society A: Mathematical, Physical and Engineering Sciences* 368, no. 1929 (2010): 4829–4850.

15. Stiesdal, "Sliding Bearing Arrangement for a Wind Turbine," US20170260970A1.

16. Daido Metal, "Newly Developed Products – Bearings for Wind Power Generation," (2025), https://www.daidometal.com/wind-power/.

17. Waukesha Bearings, "Wind: Enabling Decarbonization Through Wind Energy," (2025), https://www.waukbearing.com/en/sustainability/wind.html.

18. RENK GmbH, "Slide Bearing Technology," (2025), https://www.renk.com/en/products/slide-bearings.

19. Miba AG, "Hydrodynamic Bearings vs. Roller Bearings: What Are the Differences & Advantages?," https://www.miba.com/en/product-areas/engine-bearings/hydrodynamic-bearings-vs-roller-bearings-differences-advantages.

20. T. Schroder, G. Jacobs, A. Rolink, and D. Bosse, ""FlexPad" – Innovative Conical Sliding Bearing for the Main Shaft of Wind Turbines," *Journal of Physics: Conference Series* 1222 (2019): 012026.

21. J. Euler, G. Jacobs, A. Loriemi, T. Jakobs, A. Rolink, and J. Roder, "Scaling Challenges for Conical Plain Bearings as Wind Turbine Main Bearings," *Wind* 3, no. 4 (2023): 485–495.

22. B. Unlu and E. Atik, "Determination of Friction Coefficient in Journal Bearings," *Materials & Design* 28, no. 3 (2007): 973–977.

23. NTN, "Rolling Bearings Handbook," (2025), https://www.ntn-snr.com/sites/default/files/2017-03/rolling_bearings_handbook_en.pdf.

24. T. Hagemann, P. Pfeiffer, and H. Schwarze, "Measured and Predicted Operating Characteristics of a Tilting-Pad Journal Bearing With Jacking-Oil Device at Hydrostatic, Hybrid, and Hydrodynamic Operation," *Lubricants* 6, no. 3 (2018): 81.

25. J. Takabi and M. Khonsari, "On the Thermally-Induced Seizure in Bearings: A Review," *Tribology International* 91 (2015): 118–130.

26. Y. Wang, C. Zhang, Q. Wang, and C. Lin, "A Mixed-TEHD Analysis and Experiment of Journal Bearings Under Severe Operating Conditions," *Tribology International* 35, no. 6 (2002): 395–407.

27. S. Poddar and N. Tandon, "Study of Oil Starvation in Journal Bearing Using Acoustic Emission and Vibration Measurement Techniques," *Journal of Tribology* 142, no. 12 (2020): 121801.

28. C. Laubichler, C. Kiesling, M. da Silva, A. Wimmer, and G. Hagar, "Data-Driven Sliding Bearing Temperature Model for Condition Monitoring in Internal Combustion Engines," *Lubricants* 10, no. 5 (2022): 10050103.

29. H. Heshmat and O. Pinkus, "Performance of Starved Journal Bearings With Oil Ring Lubrication," *Journal of Tribology* 107, no. 1 (1985): 23–31.

30. S. Glavtskih, D. McCarthy, and I. Sherrington, "Hydrodynamic Performance of a Thrust Bearing With Micropatterned Pads," *Tribology Transactions* 48, no. 4 (2005): 492–498.

31. D. Lee, K. Sun, B. Kim, and D. Kang, "Thermal Behaviour of a Worn Tilting Pad Journal Bearing: Thermohydrodynamic Analysis and Pad Temperature Measurement," *Tribology Transactions* 61, no. 6 (2018): 1074–1083.

32. D. Garner and A. Leopard, "Temperature Measurements in Fluid Film Bearings," Proceedings of the 13th Turbomachinery Symposium, (1985), https://hdl.handle.net/1969.1/163655.

33. American Petroleum Institute, "API Standard 670: Machinery Protection Systems," (2014).

34. C. Ettles, R. Knox, J. Ferguson, and D. Horner, "Test Results for PTFE-Faced Thrust Pads, With Direct Comparison Against Babbitt-Faced Pads and Correlation With Analysis," *Journal of Tribology* 125, no. 4 (2003): 814–823.

35. S. Glavatskih, "Evaluating Thermal Performance of PTFE-Faced Tilting Pad Thrust Bearing," *Journal of Tribology* 125, no. 2 (2003): 319–324.

36. S. Glavatskih, "A Method of Temperature Monitoring in Fluid Film Bearings," *Tribology International* 37, no. 2 (2004): 143–148.

37. Y. Sumi, T. Sano, T. Shinohara, et al., "Development of Thrust Bearings With High Specific Load," Proceedings of ASME Turbo Expo 2014: Turbine Technical Conference and Exposition 2014, (2014), https://asmedigitalcollection.asme.org/GT/proceedings-pdf/GT2014/45585/V01BT27A044/2422778/v01bt27a044-gt2014-26798.pdf.

38. D. Henssler, L. Schneider, S. Gassmann, and T. Felix, "Qualification and Optimization of Solid Polymer Tilting-Pad Bearings for Subsea Pump Applications," 44th Turbomachinery & 31st Pump Symposia 2015, (2015), https://oaktrust.library.tamu.edu/server/api/core/bitstreams/606604a7-6bdd-4ee0-b547-e20426439496/content.

39. J. Zhou, B. Blair, J. Argires, and D. Pitsch, "Experimental Performance Study of a High Speed Oil Lubricated Polymer Thrust Bearing," *Lubricants* 3, no. 1 (2015): 3–13.

40. J. Paeβens, K. Kratz, T. Gemmeke, et al., "Design of a Fully Integrated Sensor System of a Plain Bearing," *Engineering Research* 88, no. 1 (2024): 17.

41. J. Shen, X. Xiong, G. Li, X. Wang, Z. Hua, and Z. Nie, "Experimental Analysis of Dynamic Oil Film Pressure of Tilting-Pad Journal Bearings," *Tribology Letters* 63, no. 3 (2016): 36.

42. L. Andres, H. Jani, H. Kaizar, and M. Thorat, "On the Effect of Supplied Flow Rate to the Performance of a Tilting-Pad Journal Bearing – Static Load and Dynamic Force Measurements," *Journal of Engineering for Gas Turbines and Power* 142, no. 12 (2020): 121006.

43. T. Hagemann, S. Kukla, and H. Schwarze, "Measurement and Prediction of the Static Operating Conditions of a Large Turbine Tilting-Pad Bearing Under High Circumferential Speeds and Heavy Loads," Proceedings of ASME Turbo Expo 2013: Turbine Technical Conference and Exposition 2013, (2013).

44. L. Andres, J. Yang, and A. Devitt, "On Tilting pad Carbon-Graphite Porous Journal Bearings: Measurements of Imbalance Response and Comparison to Predictions of Bearing Performance and System Dynamic Response," *Tribology Transactions* 64, no. 6 (2021): 981–995.

45. H. Ha, H. Kim, and K. Kim, "Inlet Pressure Effects on the Thermohydrodynamic Performance of a Large Tilting Pad Journal Bearing," *Journal of Tribology* 117, no. 1 (1995): 160–165.

46. S. Yang, C. Kim, and Y. Lee, "Experimental Study on the Characteristics of Pad Fluttering in a Tilting Pad Journal Bearing," *Tribology International* 39, no. 7 (2006): 686–694.

47. R. Dwyer-Joyce, B. Drinkwater, and C. Donohoe, "The Measurement of Lubricant-Film Thickness Using Ultrasound," *Proceedings of the Royal Society of London, Series A: Mathematical, Physical and Engineering Sciences* 459, no. 2032 (2003): 957–976.

48. R. Dwyer-Joyce, P. Harper, and B. Drinkwater, "A Method for the Measurement of Hydrodynamic Oil Films Using Ultrasonic Reflection," *Tribology Letters* 17, no. 2 (2004): 337–348.

49. T. Reddyhoff, R. Dwyer-Joyce, and P. Harper, "Ultrasonic Measurement of Film Thickness in Mechanical Seals," *Sealing Technology* 2006, no. 7 (2006): 7–11.

50. R. Dwyer-Joyce, P. Harper, J. Pritchard, and B. Drinkwater, "Oil Film Measurement in Polytetrafluoroethylene-Faced Thrust Pad Bearings for Hydrogenator Applications," *Proceedings of the Institution of Mechanical Engineers, Part A: Journal of Power and Energy* 220, no. 6 (2006): 619–628.

51. R. Mills, J. Vail, and R. Dwyer-Joyce, "Ultrasound for the Non-Invasive Measurement of Internal Combustion Engine Piston Ring Oil Films," *Proceedings of the Institution of Mechanical Engineers, Part J: Journal of Engineering Tribology.* 229, no. 2 (2015): 207–215.

52. S. Beamish, X. Li, H. Brunskill, A. Hunter, and R. Dwyer-Joyce, "Circumferential Film Thickness Measurement in Journal Bearings via the Ultrasonic Technique," *Tribology International* 148 (2020): 106295.

53. S. Beamish and R. Dwyer-Joyce, "Experimental Measurements of Oil Films in a Dynamically Loaded Journal Bearings," *Tribology Transactions* 65, no. 6 (2022): 1022–1040.

54. D. McCarthy, S. Glavatskih, and I. Sherrington, "Oil-Film Thickness and Temperature Measurements in PTFE and Babbitt Faced Tilting-Pad Thrust Bearings," *Proceedings of the Institution of Mechanical Engineers, Part J: Journal of Engineering Tribology* 219, no. 3 (2005): 179–185.

55. G. Pitts, "The Steady State Characteristics of the Tilting-Pad Gas-Journal Bearing" (PhD thesis, 1967).

56. F. Cangioli, R. Livermore-Hardy, G. Pethybridge M. Uemit, M. Stottrop, and B. Bender, "Experimental Investigation and Numerical Modelling of a Large Heavily-Loaded Tilting Pad Journal Bearing With Polymer Lined Pads," Proceedings of ASME Turbo Expo 2020, (2020).

57. M. Stottrop, A. Engels, C. Weiβbacher, and B. Bender, "Experimental Investigation of a Large Tilting-Pad Journal Bearing With a Direct-Bonded Sub-Millimeter Peek Lining," Proceedings of ASME Turbo Expo 2023, (2023).

58. T. Hagemann, D. Vetter, S. Wettmarshausen, et al., "A Design for High-Speed Journal Bearings With Reduced Pad Size and Improved Efficiency," *Lubricants* 10, no. 313 (2022): 10110313.

59. "Micro-Epsilon Catalogue," (2025), https://www.micro-epsilon.co.uk/fileadmin/download/products/cat--capaNCDT--en.pdf.

60. "Micro-Epsilon Eddy Current Sensor Catalogue," (2025), https://www.micro-epsilon.co.uk/fileadmin/download/products/cat--eddyNCDT--en.pdf.

61. S. Glavatskih, O. Uusitalo, and D. Spohn, "Simultaneous Monitoring of Oil Film Thickness and Temperature in Fluid Film Bearings," *Tribology International* 34, no. 12 (2001): 853–857.

62. F. Zhang, W. Ouyang, H. Hong, Y. Guan, X. Yuan, and G. Dong, "Experimental Study on Pad Temperature and Film Thickness of Tilting-Pad Journal Bearings With an Elastic-Pivot Pad," *Tribology International* 88 (2015): 228–235.

63. C. Mahieux, "Experimental Characterization of the Influence of Coating Materials on the Hydrodynamic Behaviour of Thrust Bearings: A Comparison of Babbitt, PTFE, and PFA," *Journal of Tribology* 127, no. 3 (2005): 568–574.

64. A. Schubert and T. Brescianini, "Application of PEEK Coated Thrust Bearing on the Occasion of a Refurbishment of a Large Hydro Power Plant With Concurrent Load Increase," Proceedings of 10th EDF/Prime Poitiers Workshop (2011).

65. P. Dang, S. Chatterton, and P. Pennacchi, "Static Characteristics of a Tilting Five-Pad Journal Bearing With an Asymmetric Geometry," *Actuators* 9, no. 3 (2020): 9030089.

66. E. Ciulli, R. Ferraro, P. Forte, A. Innocenti, and M. Nuti, "Experimental Characterization of Large Turbomachinery Tilting Pad Journal Bearings," *Machines* 9, no. 273 (2021): 9110273.

67. G. Daiki, I. Tsuyoshi, H. Takekiyo, et al., "Failure Diagnosis and Physical Interpretation of Journal Bearing for Slurry Liquid Using Long-Term Real Vibration Data," *Structural Health Monitoring* 23, no. 2 (2024): 1201–1216.

68. GyroMetric systems, "Bearing Monitoring," (2025), https://gyrometric.systems/ime-bearing-monitoring/.

69. D. Tschoepe and D. Childs, "Measurements Versus Predictions for the Static and Dynamic Characteristics of a Four-Pad, Rocket-Pivot, Tilting-Pad Journal Bearing," *Journal of Engineering for Gas Turbines and Power* 136, no. 5 (2014): 052501.

70. P. Zemella, T. Hageman, B. Pfau, and H. Schwarze, "Identification of Dynamic Coefficients of a Five-Pad Tilting Pad Journal Bearing up

to Highest Surface Speeds," *Journal of Engineering for Gas Turbines and Power* 143, no. 8 (2021): 081013.

71. P. Dang, S. Chatterton, P. Pennacchi, and A. Vania, "Effect of the Load Direction on Non-Nominal Five-Pad Tilting-Pad Journal Bearings," *Tribology International* 98, no. 98 (2016): 197–211.

72. L. Andres and O. Santiago, "Imbalance Response of a Rotor Supported on Flexure Pivot Tilting Pad Journal Bearings in Series With Integral Squeeze Film Dampers," *Journal of Engineering for Gas Turbines and Power* 125, no. 4 (2003): 1026–1032.

73. R. Kawashita, T. Nishioka, S. Yokoyama, M. Iwasaki, S. Isayama, and Y. Waki, "Study on Subsynchronous Vibration With Tilting Pad Journal Bearing Under Starved Lubrication," ASME Turbo Expo 2018: Turbomachinery Technical Conference and Exposition, (2018).

74. M. Huang, L. Jiang, P. Liaw, C. Brooks, R. Seeley, and D. Klarstrom, "Using Acoustic Emission in Fatigue and Fracture Materials Research," *Journal of the Minerals, Metals & Materials Society* 50, no. 11 (1998): 1–14.

75. Y. Feng, Y. Chen, N. Yu, F. Meng, Q. Jia, and X. Yuan, "Experimental Study on Rubbing Failure of Tilting Pad Bearing in Heavy Duty Gas Turbine," 2022 *Global Reliability and Prognostics and Health Management*, (2022).

76. F. Konig, J. Marheineke, G. Jacobs, C. Sous, M. Zuo, and Z. Tian, "Data-Driven Wear Monitoring for Sliding Bearings Using Acoustic Emission Signals and Long Short-Term Memory Neural Networks," *Wear* 476 (2021): 203616.

77. S. Poddar and N. Tandon, "Classification and Detection of Cavitation, Particle Contamination and Oil Starvation in Journal Bearing Through Machine Learning Approach Using Acoustic Emission Signals," *Proceedings of the Institution of Mechanical Engineers, Part J: Journal of Engineering Tribology* 235, no. 10 (2021): 2137–2143.

78. G. Zhang, Z. Liu, X. Wang, and H. Xu, "Experimental Study of Tilting Pad Journal Bearing-Rotor System With Acoustic Emission Technique," *Proceedings of the Institution of Mechanical Engineers, Part J: Journal of Engineering Tribology* 224, no. 1 (2009): 115–122.

79. M. Nagata, M. Fujita, M. Yamada, and T. Kitahara, "Evaluation of Tribological Properties of Bearing Materials for Marine Diesel Engines Utilizing Acoustic Emission Technique," *Tribology International* 46, no. 1 (2012): 183–189.

80. J. Zhou and B. Blair, "Bearing Monitoring/Analysis System," US11255750B2.

81. G. Tian, Z. Zhao, and R. Baines, "The Research of Inhomogeneity in Eddy Current Sensors," *Sensors and Actuators A* 69 (1998): 148–515.

82. I. Adewale and G. Tian, "Decoupling the Influence of Permeability and Conductivity in Pulsed Eddy-Current Measurements," *IEEE Transactions on Magnetics* 49, no. 3 (2013): 1119–1127.

83. Y. Yu, G. Tian, X. Li, and A. Simm, "An Approach to ERO Problem in Displacement Eddy Current Sensor," *Nondestructive Testing and Evaluation* 28, no. 3 (2013): 195–207.

84. K. Kinnunen, "Electrical Runout in Eddy Current Displacement Measurement" (master's thesis, 2022).

85. M. Nasselqvist, R. Gustavsson, and J. Aidanpaa, "Bearing Load Measurement in a Hydropower Unit Using Strain Gauges Installed Inside Pivot Pin," *Experimental Mechanics* 52 (2012): 361–369.

86. R. Gustavsson, M. Lundstrom, and J. Aidanpaa, "Determination of Journal Bearing Stiffness and Damping at Hydropower Generators Using Strain Gauges," ASME 2005 Power Conference, (2008).

87. Z. Yao, Q. Zhang, Y. Tao, and X. Zhang, "A New Approach to Measure the Friction Coefficient of Micro Journal Bearings," *Tribology International* 33, no. 7 (2000): 485–489.

88. M. Stansloski, A. Neumeier, and G. Slinger, "Strain Gage Based System and Method for Failure Detection of a Fluid Film Bearing," US20160356657A1.

89. REOTEMP Instrument Corporation, "Thermocouple Accuracies," (2025), https://www.thermocoupleinfo.com/thermocouple-accuracies.htm.

90. Omega, "Temperature Probes," (2025), https://www.omega.co.uk/temperature/z/thermocouple-RTD.html.

91. Boiswood Ltd, "Capacitive Pressure Sensors," (2025), https://www.boiswood.co.uk/blog/capacitive-pressure-sensors#:~:text=High%20Accuracy%20%2D%20up%20to%20%C2%B1,accurate%20over%20the%20long%20haul.

92. Kistler, "Kistler M6 Absolute Pressure Transducer," (2025), https://kistler.cdn.celum.cloud/SAPCommerce_Download_original/003-391e.pdf.

93. Kistler, "Piezoelectric Pressure Sensor for Test & Measurement Applications," (2025), https://kistler.cdn.celum.cloud/SAPCommerce_Download_original/003-288e.pdf.

94. M. Kaneta, T. Sakai, and H. Nishikawa, "Optical Interferometric Observations of the Effects of a Bump on Point Contact EHL," *Journal of Tribology* 114, no. 4 (1992): 779–784.